

Polymerization Mechanism of Di(benzylidene)tetrathiapentalenes into Linearly Extended TTF Polymers

Philippe Hapiot,^{1a} Fouad Salhi,^{1b} Bernadette Divisia-Blohorn,^{1c} and Harald Müller*^{1b}

Laboratoire d'Electrochimie Moléculaire de l'Université Denis Diderot-Paris 7, UMR 7591 (Université/CNRS), 2 place Jussieu, Case Courrier 7107, 75251 Paris Cedex 05, France, European Synchrotron Radiation Facility (ESRF), B.P. 220, 38043 Grenoble Cedex 09, France, and Laboratoire d'Electrochimie Moléculaire et Structures des Interfaces, UMR 5819 (CEA/CNRS/Université Grenoble 1), Département de Recherche Fondamentale sur la Matière Condensée, CEA-Grenoble, 17 rue des Martyrs, 38054 Grenoble Cedex 09, France

Received: April 14, 1999; In Final Form: October 6, 1999

The mechanism of the oxidative polymerization of di(benzylidene)tetrathiapentalenes (R-DBTTP; where R = H, OCH₃, CF₃) into linearly extended TTF polymers has been investigated by cyclic voltammetry at low and high scan rates. The polymerization involves as a first step the formation of the monomer radical cations which undergo rapidly a radical dimerization reaction. The dimerization rate constants were found to be in the range of $2k_{\text{dim}} = 4 \times 10^6$ to 10^7 L mol⁻¹ s⁻¹. The dimerization products slowly deprotonate to give the corresponding vinylogous tetrathiafulvalene (TTF) derivatives ($k_{\text{H}} = 0.02$ – 10 s⁻¹). Polymerization only occurs, if the TTF intermediates are oxidized to the radical trication, a behavior which sharply contrasts the known electropolymerization mechanism of pyrrole or thiophene.

Introduction

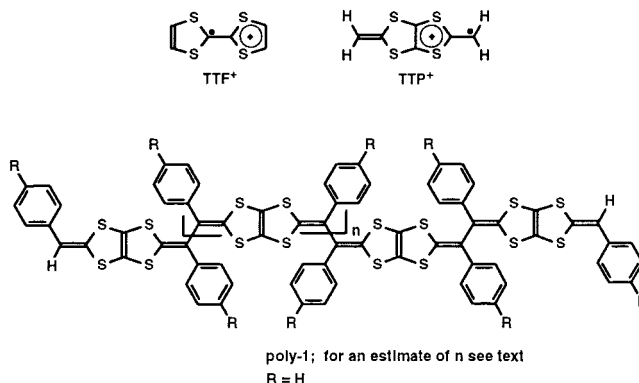
The π -electron donor tetrathiafulvalene (TTF) and its derivatives are the key building blocks in the rapidly evolving field of molecular conductors. Owing to the exciting solid-state properties of their radical cation salts, such as high electrical conductivity or even superconductivity, TTF and its derivatives have been the focus of general interest for more than 2 decades.^{2,3} The potential technological applications of these materials have spurred numerous attempts to incorporate TTF radical salts into polymeric backbones to combine their electrical conductivity with the enhanced processability of macromolecular structures. To date, the polymeric TTF derivatives described in the literature have been prepared from functionalized TTF monomers and consist of essentially independent TTF moieties attached to a polymeric backbone or of segregated TTF units linked through suitable spacer groups.⁴

Recently, the synthesis of a series of bis-substituted tetrathiapentalenes has been reported with the objective of employing these compounds as precursors for the preparation of linearly extended TTF oligo- and polymer derivatives by oxidative radical coupling.⁵ Linear fusion of TTF units could offer a promising approach to stabilize metallic conductivity in oligo- and polymeric TTF derivatives.⁶

The synthetic strategy takes advantage of the fact that the oxidation of TTF leads generally to stable radical cations, whereas the radical cation of hypothetical, iso- π -electronic 1,3,4,6-tetrathiapentalene (TTP) is expected to be highly reactive⁷ (cf. Chart 1). Very recently, the one step preparation of the first linearly annelated TTF polymer (poly-1, see Chart 1) starting from a TTP precursor could be realized successfully.⁸

A detailed understanding of the individual reaction steps involved in the oligo- and polymerization of TTP is not only

CHART 1: General Formula of the Radical Cations of Tetrathiafulvalene (TTF) and Tetrathiapentalene (TTP) (Top) and of the Neutral Polymer Poly-1 (Bottom)



of considerable interest for the accurate control of the polymerization conditions but also of fundamental importance as a preparative coupling reaction involving C–C bond formation.⁹

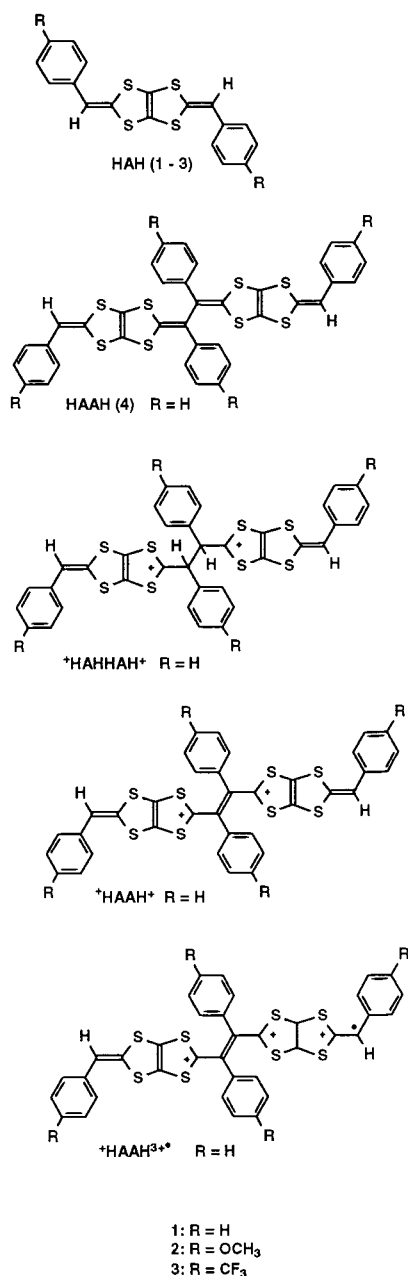
We present hereafter a detailed study of the oxidative oligo- and polymerization mechanism of para-disubstituted 2,5-di(R-benzylidene)-1,3,4,6-tetrathiapentalenes (R-DBTTP; R = H, OCH₃, CF₃; **1**–**3**) by classical as well as ultrafast cyclic voltammetry. In the text and Charts 1 and 2, a simplified notation will be used. The monomer will be referred to as HAH, the corresponding dimer as HAAH. For simplicity, the structural formulas shown in the charts are based on the *trans* (*E*) conformation of R-DBTTP.

Experimental Section

Chemicals. CH₂Cl₂ was of spectroscopy grade and used as received (Merck). The supporting electrolyte *n*-NBu₄PF₆ as well

* Corresponding author. Phone: 33-47688-2484. Fax: 33-47688-2542. E-mail: mueller@esrf.fr.

CHART 2: General Formula of 2,5-di(R-benzylidene)-1,3,4,6-tetrathiapentalenes (HAH; R = H, OCH₃, CF₃; 1–3), Dimer 4 (HAAH; R = H), and of the Various Intermediates



as the proton acceptor 2,6-lutidine (2,6-dimethylpyridine) were purchased from Fluka (both puriss. p.a.) and used without further purification. R-DBTTP and the vinyllogous TTF derivative 1,2-bis(5-benzylidene[1,3]dithiolo[4,5-*d*]1,3-dithiole-2-ylidene)-1,2-diphenylethane (**4**) were prepared as described previously.⁵ R-DBTTP were obtained as mixtures of *cis* and *trans* (*E/Z*) isomers and used as such.

Solutions were always prepared freshly before experiments; dissolved oxygen was removed by bubbling argon through the solutions.

Electrochemical Experiments. All the cyclic voltammetry experiments were carried out at 20 ± 0.1 °C using a cell equipped with a thermostated jacket. The counter electrode was a Pt wire, and the reference electrode was an aqueous saturated calomel electrode (SCE; $E^\circ/\text{SCE} = E^\circ/\text{NHE} - 0.2412$ V) with a salt bridge containing the supporting electrode. The SCE was

checked against the ferrocene/ferricinium couple in CH₂Cl₂/0.1 M *n*-NBu₄PF₆ ($E^\circ = +0.528$ V/SCE) before and after each experiment.

For low scan rate cyclic voltammetry (0.05–500 V s⁻¹), the working electrodes were either disks of glassy carbon (Ø 0.8 mm, Tokai Corp.), gold (Ø 1 mm) or platinum (Ø 1 mm and Ø 3 mm, respectively). The electrodes were carefully polished before each set of voltammograms with 1 μm diamond paste and cleansed in an ultrasonic bath with absolute ethanol. The electrochemical instrumentation consisted of a PAR model 175 Universal programmer and of a home-built potentiostat equipped with a positive feedback compensation device.¹⁰ The data were acquired with a 310 Nicolet oscilloscope.

For high scan rate cyclic voltammetry, the ultramicroelectrodes were gold or platinum wires (Ø 10 μm) sealed in soft glass.¹¹ The signal generator was a Hewlett-Packard 3314A and the curves were recorded with a 4094C Nicolet oscilloscope with a minimum acquisition time of 5 ns per point.

Simulations of the cyclic voltammograms were made with Digisim 2.1, "A cyclic voltammetric simulator for Windows", Bioanalytical Systems Inc.

Results and Discussion.

Redox Behavior of the Monomers 1–3. Electrochemical investigations were performed by cyclic voltammetry on working electrodes made from platinum, gold, and glassy carbon, respectively. The different electrode materials gave comparable results, thus indicating that their nature does not influence significantly the electrode reactions.

The electrochemical behavior of the R-DBTTP investigated is very similar; therefore, only that of H-DBTTP (**1**) will be discussed in detail as a representative example. At low scan rate (0.1 V s⁻¹) and during the first anodic scan, **1** exhibits an irreversible one-electron peak I at a peak potential $E_p^I = 0.78$ V,¹⁴ assignable to the formation of the radical cation HAH^{•+}. The first one-electron transfer is followed by a second irreversible wave II at a peak potential $E_p^{II} = 1.35$ V (see the first cycle of Figure 1a) which involves the transfer of more than one electron.¹³ This indicates follow-up reactions of the radical species HAH^{•+} on the time scale of the voltammetric experiment.

The observation of a reversible redox signal for the first electron-transfer process requires an increase of the scan rate ν to 1000 V s⁻¹. Accordingly, the lifetime of HAH^{•+} can be estimated to be on the order of tenths of milliseconds. Cyclic voltammograms (CVs) of compound **1**, recorded at scan rates of 0.2 and 2400 V s⁻¹, are displayed in parts a and c of Figure 2, respectively.

CVs of **1** show at $\nu = 0.1$ V s⁻¹ and starting with the second subsequent cycle, the appearance of new peaks in addition to peak I (oxidation peak I', reduction peaks III and IV, Figure 1b). These peaks point to the formation of a new electroactive species from HAH^{•+}. The reduction peaks III and IV disappeared completely after homogenization of the solution with argon bubbling and suggest the presence of a soluble product. Peak I' is small, however, and does not increase significantly with subsequent scans thus pointing to a rather slow follow-up reaction of HAH^{•+} (several seconds) under these conditions. Interestingly, peak I' appears in a potential region where HAAH, the *stable* dimerization product of **1**, exhibits two reversible redox waves (*vide infra*).

When the switching potential was set to a value more positive than E_p^{II} (about +1.6 V vs SCE), a completely different electrochemical behavior was observed. The multisweep CV

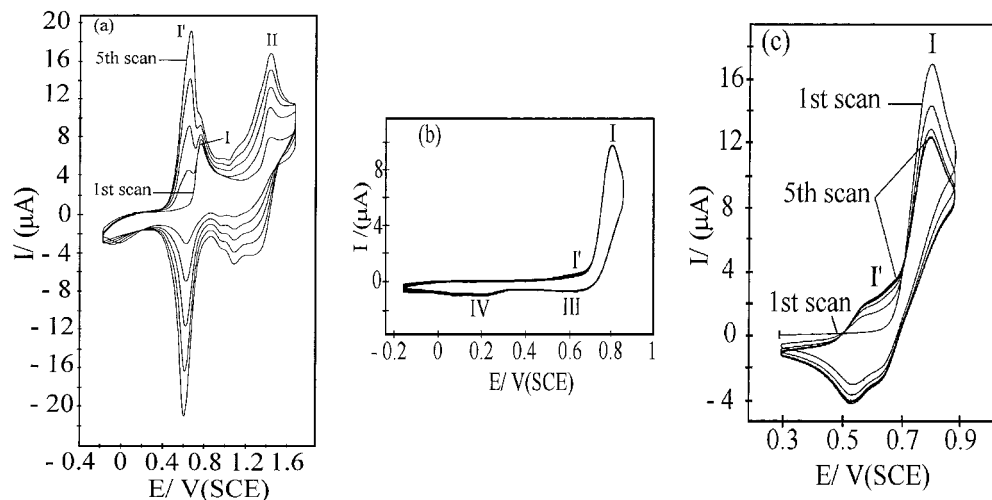


Figure 1. Multisweep cyclic voltammogram of H-DBTTP (**1**) (1.5×10^{-4} M in CH_2Cl_2 + 0.1 M $n\text{-Bu}_4\text{NPF}_6$; Pt disk electrode \varnothing 3 mm at $\nu = 0.1$ V s^{-1}): (a and b) without added base; (c) after addition of an equimolar amount of 2,6-lutidine.

of H-DBTTP (Figure 1a) reveals the evolution of the symmetrical redox wave I' at a peak potential more negative than E_p^1 . Simultaneously, anodic and cathodic peak currents increase with each subsequent scan, thus evidencing the deposition of an electroactive species on the working electrode. The shape and the peak positions of the CV remained essentially unchanged after the working electrode with the adhering deposit was transferred into a blank, monomer-free electrolyte, a behavior in accordance with the formation of a surface-immobilized species. Continued potential cycling (500 cycles) between 0 and +1.6 V vs SCE or potentiostatic electrolysis at +1.6 V vs SCE allowed to deposit black films on the working electrode (cf. Chart 1). The correspondence of the electropolymerization product described here and authentic poly-**1** obtained by treatment of **1** with nitrosonium hexafluorophosphate was ascertained by FT-IR and ESR spectroscopy. The number n of repetitive monomer units amounts at least to eight; the lower limit of the molecular weight corresponds to 2836 g mol^{-1} (without counterions) as determined by FAB and MALDI-TOF mass spectrometry. A more complete account of the characterization of poly-**1** has been given elsewhere.⁸

Oxidation Potential of Monomers and Polymers. The standard oxidation potentials E° for the redox couple $\text{HAH}/\text{HAH}^{+\bullet}$ were derived from the reversible voltammograms recorded at high scan rate as the half-sum of the forward and the backward peak potentials (see Figure 2b). For comparison, the half-sum potentials $E_{1/2}$ for the corresponding polymers were determined at low scan rate. The symmetrical shapes of anodic and cathodic peaks as well as the small peak separations ($\Delta E_p \cong 40\text{--}60$ mV) indicate that the latter values are not far from thermodynamic equilibrium and thus allow the determination of E° for the electrodeposited polymers (cf. Table 1).

As expected, the oxidation potentials of R-DBTTP depend on the nature of the substituents R. The presence of electron-donating methoxy groups results in a slightly lower oxidation potential for $\text{CH}_3\text{O-DBTTP}$ with regard to H-DBTTP, whereas the presence of electron-withdrawing trifluoromethyl groups in $\text{CF}_3\text{-DBTTP}$ leads to a significant enhancement of E° .

The variation of the standard oxidation potential with the Brown coefficient σ^+ for R-DBTTP and poly-**1** to poly-**3** is displayed in Figure 3. For the monomers a linear variation of E° with σ^+ is observed.¹⁴ The corresponding slope ρ_+ amounts to a value of 0.17, whereas the linear fit for the polymer series gives a value of 0.06. The larger slope found for the monomer oxidation potentials indicates a strong interaction of the charge

on the 1,3-dithiole units with the phenyl substituents. Such view is in agreement with the fact that well-defined, reversible CVs of all R-DBTTP with a small peak potential separation $\Delta E_p = 105$ mV could be obtained at high scan rate ($\nu = 2400$ V s^{-1}). This corresponds to a standard heterogeneous electron-transfer rate constant $k_s \geq 1.0$ cm s^{-1} for R-DBTTP,¹⁵ a value similar to those found for electrochemical systems with fast electron transfer.¹⁶ The large k_s values are suggestive of a low solvent reorganization energy upon electron transfer and point to a charge delocalization over the whole molecule. Following this line of reasoning, it may further be concluded that the smaller slope found for poly-**1** to poly-**3** results from a spreading of positive charge mainly along the conjugated polymer chain with little participation of the phenyl substituents. It is well possible that the dihedral twist angles between the terminal phenyl substituents and the central TTP moieties of R-DBTTP and those of the internal phenyl substituents of the corresponding polymers differ significantly. A considerable increase of the twist angles in the polymers would be an effective way to reduce charge delocalization between polymer chain and substituents and could thus account for the behavior observed.¹⁷

Polymerization Mechanism. The oxidative polymerization of R-DBTTP occurs in several subsequent steps. The proposed mechanism involves as initial steps the oxidation of the monomer HAH to the radical cation $\text{HAH}^{+\bullet}$, followed by radical-radical (or radical-substrate) coupling to $^+\text{HAHHAH}^+$ with subsequent proton abstraction to the vinylogous TTF derivative HAAH. In a previous report on the oxidative dimerization of 1,4-dithiafulvenes, a class of compounds closely related to the monomeric precursors studied here, it was found that dimer formation involved a fast coupling reaction between two radical cations, followed by slow deprotonation of the coupling product.⁹ To elucidate whether a similar radical-radical coupling reaction is involved in the oxidation of R-DBTTP, the variation of E_p^1 with ν was investigated. For all three monomers, a linear variation of E_p^1 with the logarithm of ν was observed with slopes $\delta(E_p^1)/\delta(\log \nu)$ of around 20 mV, when ν was altered between 0.05 and 50 V s^{-1} ¹⁸ (see Table 1). In view of the very similar values, it may be concluded that the same mechanism applies for the oxidation of all three compounds. Such values are in agreement with a mechanism involving a fast electron transfer to form $\text{HAH}^{+\bullet}$, followed by a radical-radical dimerization leading to $^+\text{HAHHAH}^+$ as exemplified in the scheme.¹⁸ The presence of a radical-substrate coupling mechanism appears highly unlikely but cannot be

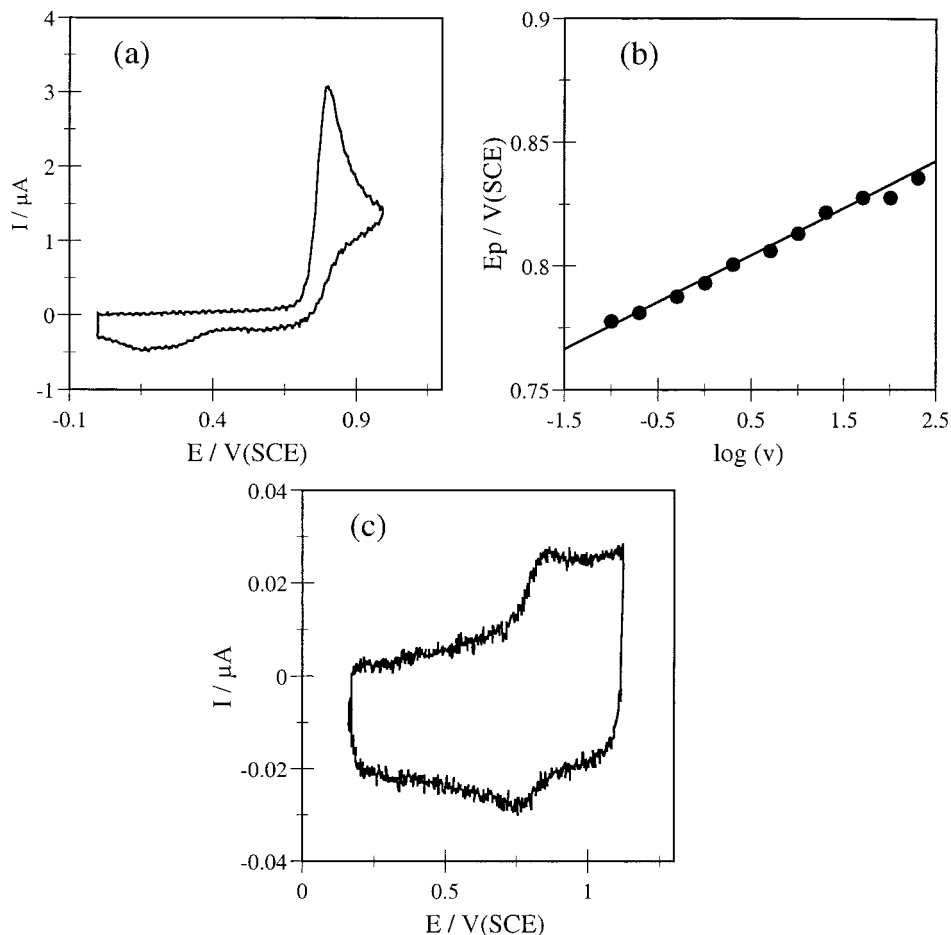


Figure 2. Cyclic voltammogram of H-DBTTP (**1**) (5×10^{-4} M in CH_2Cl_2 + 0.1 M *n*-Bu₄NPF₆; Pt disk electrode \varnothing 1 mm): (a) at $\nu = 0.2$ V s⁻¹ (c) at $\nu = 2400$ V s⁻¹. (b) Variation of the peak potential E_p^1 with the logarithm of ν .

TABLE 1: Electrochemical Oxidation of R-DBTTP

compound R	$E_{\text{R-DBTTP}}^{\circ}$ (V/SCE) ^a	$\delta E_p^1/\delta(\log \nu)$ ^b (mV)	$2k_{\text{dim}}^c$ (L mol ⁻¹ s ⁻¹)	k_{H}^c (s ⁻¹)	$E_{1/2}^{\text{polymer}^d}$ (V/SCE) ^e
-H	0.805	19.7	8×10^6	0.02	0.62
-OCH ₃	0.693	19.2	4×10^6	10	0.60
-CF ₃	0.941	20.0	10^7	0.5	0.69

^a Error \pm 10 mV. ^b On platinum electrode. ^c Error \pm a factor of 2. ^d $E_{1/2} = (E_p^{\text{ox}} + E_p^{\text{red}})/2$. ^e Error \pm 20 mV.

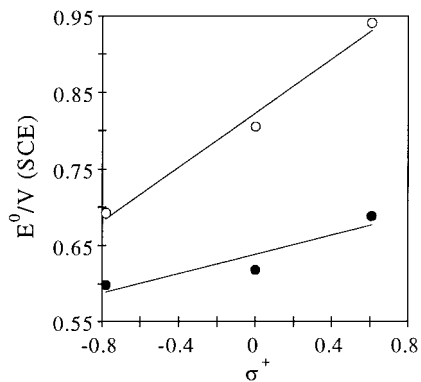


Figure 3. Variation of the oxidation potentials E° of R-DBTTP (**1-3**) (○) and poly-**1** to poly-**3** (●) as a function of the Brown coefficient σ^+ .

excluded completely. A study of the dependence of E_p^1 on the initial concentration of R-DBTTP and ν , needed for an accurate distinction between both theoretically possible mechanisms, is precluded by the unusually low solubility of R-DBTTP in common organic solvents.

A comparison of the experimental CVs with curves calculated for the radical-radical coupling mechanism allows the dimerization rate constant, $2k_{\text{dim}}$, to be determined. The values of $2k_{\text{dim}}$ range from 4×10^6 to 10^7 L mol⁻¹ s⁻¹ and are comparable within experimental accuracy (cf. Table 1); the nature of the substituents appears to be of little, if any, significance.

The kinetics of the dimer formation appears to be rather slow, an observation in apparent disagreement with the short lifetime of the initially produced HAH^{•+}. In view of the large dimerization constant $2k_{\text{dim}}$, such behavior could indicate that a fast dimerization leading to unstable ⁺HAHHAH⁺ is followed by a slow deprotonation to HAAH.

To study the influence of the proton transfer on the global kinetics, the effect of added base on the electrochemical behavior was investigated. Multisweep CVs of monomer **1**, recorded without and with the addition of 2,6-lutidine, but otherwise identical experimental conditions, are displayed in parts b and c of Figure 1, respectively. The peak current of the oxidation wave I grows considerably from a relative value of 1 to about 1.7 in the presence of an equimolar amount of 2,6-lutidine (1.5×10^{-4} mol L⁻¹), whereas the reduction peak IV disappears completely upon addition of base. Such behavior makes plausible an interpretation of wave IV as reduction of ⁺HAHHAH⁺ (not shown in Figure 1c). Taking into account the fact that HAAH can be oxidized readily to ⁺HAAH⁺ at the potential required to generate HAH^{•+}, the total number of electrons exchanged per mole of HAAH is expected to pass from 1 to 2 as the deprotonation rate of ⁺HAHHAH⁺ increases. Thus, the considerable growth of the peak currents I' and I together with the disappearance of peak IV demonstrates clearly

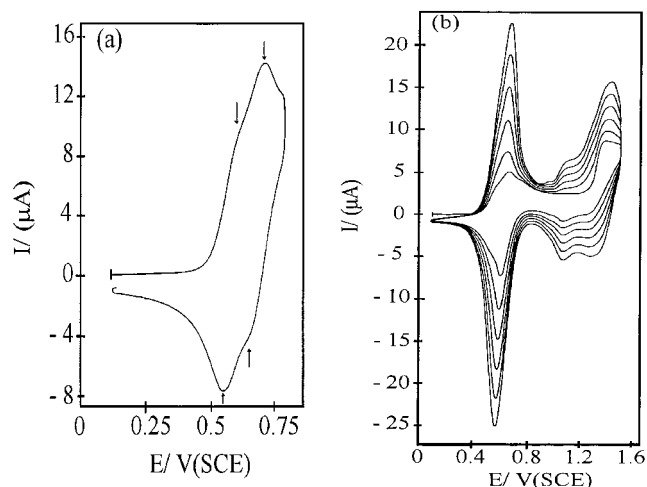


Figure 4. Cyclic voltammogram of HAAH (**4**) (5×10^{-4} M in $\text{CH}_2\text{-Cl}_2 + 0.1$ M of $n\text{-Bu}_4\text{NPF}_6$; Pt disk electrode \varnothing 1 mm at $\nu = 0.1$ V s^{-1}): (a) Single sweep between +0.1 V and +0.75 V vs SCE. (b) Multisweep between +0.1 V and +1.5 V vs SCE.

an acceleration of the dimer formation upon addition of base. This view is fully in line with the presumption of a deprotonation reaction of initially formed $^+\text{HAHHAH}^+$ to HAAH as a rate-limiting step of the overall kinetics (cf. later scheme).

Assuming that the deprotonation reaction of $^+\text{HAHHAH}^+$ occurs as a single step,¹⁹ the comparison of the experimental data with the simulated curves allows the estimation of the apparent deprotonation rate constant k_{H} to a value of around 0.02 s^{-1} in the absence of base. Similarly, a second-order rate constant of $2 \times 10^4 \text{ L mol}^{-1} \text{ s}^{-1}$ can be determined for the deprotonation of $^+\text{HAHHAH}^+$ in the presence of 2,6-lutidine. The rate constants for the monomers **2** and **3** are comparable and compiled in Table 1. The relatively small values of k_{H} confirm that the deprotonation of $^+\text{HAHHAH}^+$ is slow even in the presence of base and occurs after the irreversible radical–radical dimerization. Single or repetitive potential scans in a range confined to the one-electron oxidation of R–DPTTP (i.e., around +0.75 V vs SCE) led solely to the formation of HAAH as a stable product, whereas electrodeposition indicating polymer formation was never observed. The formation of a surface-immobilized electroactive species could only be achieved if the switching potential was set at a value more positive than the second peak potential of the monomers investigated (about +1.6 V vs SCE; compare parts a, b, and c of Figure 1, respectively, for experiments performed without or with added base).

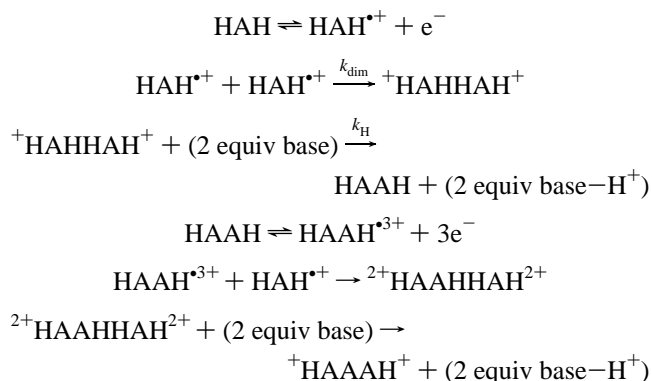
To study in more detail the reaction steps following the initial dimerization of $\text{HAH}^{\bullet+}$, the electrochemical properties of dimer **4** were investigated. The CV of authentic **4** in the potential range from 0 to +750 mV vs SCE is displayed in Figure 4a. The graph exhibits two reversible redox waves with close-lying peak potentials readily assignable to the formation of the radical cation $\text{HAAH}^{\bullet+}$ and the dication $^+\text{HAAH}^+$, respectively. The oxidation peak potentials of both anodic peaks agree well with the values assigned previously to the oxidative formation of **4** from **1** (cf. Figure 1). The standard potentials E° for the two reversible redox processes were determined to be +0.58 and +0.68 V vs SCE. Both the oxidation potentials and the reversibility of the CV are in line with the behavior expected for a vinyllogous TTF derivative.² An increase of the switching potential to +1500 mV vs SCE (cf. Figure 4b) enables the detection of a third irreversible oxidation process attributed to the formation of the radical trication $\text{HAAH}^{\bullet 3+}$. The determi-

nation of the amount of charge involved in the irreversible electron transfer by digital simulation gave values ranging from 1.65 to 1.88, indicating that further chemical reactions and electron transfers occur after the initial formation of $\text{HAAH}^{\bullet 3+}$. The accurate analysis is hampered severely by the poor resolution of the reversible pair of waves as well as by the high reactivity of $\text{HAAH}^{\bullet 3+}$. Continued potential cycling of HAAH between 0 and +1500 mV vs SCE gave rise to a CV the shape and peak positions of which are strikingly similar to that obtained from HAH after several subsequent cycles (cf. Figures 1a and 4b). Noteworthy, the formation of $\text{HAAH}^{\bullet 3+}$ requires an oxidation peak potential close to that of E_{p}^{II} observed during the oxidation of HAH. The oxidation potential of the electrodeposited material ($E_{1/2} = +0.63$ V vs SCE) obtained from HAAH is identical to that found for poly-**1** made directly from **1** (cf. Figure 4b) and thus corroborates the validity of the conclusions drawn above.

In summary, the following conclusions concerning the polymerization mechanism of R–DBTTP can be drawn: the one-electron oxidation of monomer HAH provides the highly reactive radical–cation $\text{HAH}^{\bullet+}$ which undergoes a fast dimerization reaction to the protonated dimer $^+\text{HAHHAH}^+$. The dicationic intermediate is unstable, deprotonates slowly, and gives after oxidation the stable dicationic TTF derivative $^+\text{HAAH}^+$. Polymerization only occurs if $^+\text{HAAH}^+$ is further oxidized to the radical trication $\text{HAAH}^{\bullet 3+}$, a process occurring at relatively high potential values where the oxidation peak II is observed (cf. Figure 1a). Potential cycling between 0 and +1.6 V at low scan rate, as used for polymer deposition on the anode, generates the intermediate $\text{HAAH}^{\bullet 3+}$ rapidly only in the presence of a proton acceptor, either by homogeneous or heterogeneous oxidation of $^+\text{HAAH}^+$.

Since electropolymerization experiments were always carried out in the absence of base, an additional complication must be considered. In view of the relatively small values of k_{H} , a complete deprotonation of $^+\text{HAHHAH}^+$ is unlikely on the time scale of a potential sweep from 0 to +1.6 V vs SCE (16 s for $\nu = 100$ mV/s). Therefore, it is well possible that HAHHAH is transformed directly into $\text{HAAH}^{\bullet 3+}$ in an overall transfer of three electrons and two protons. Restated in other words, the second irreversible oxidation peak II observed in the CV of monomer **1** (cf. Figure 1a) originates in fact from several, simultaneously occurring electron transfer processes of distinct redox-active species being present in solution.

Most likely, $\text{HAAH}^{\bullet 3+}$ undergoes the same type of radical–radical coupling as discussed already for the dimerization of $\text{HAH}^{\bullet+}$. Chain growth occurs either by dimerization of $\text{HAAH}^{\bullet 3+}$ or by coupling of $\text{HAAH}^{\bullet 3+}$ and $\text{HAH}^{\bullet+}$. The global polymerization mechanism is represented by the following simplified scheme:²⁰



The proposed mechanism is unusual for an oxidative polymerization process in that the polymerization does not occur at the oxidation potential of the monomer, as is typically the case for the anodic electropolymerization of pyrrole or thiophene.^{21,22} Such behavior can easily be rationalized when taking into account the hybrid character of HAAH. Depending on the potential range chosen for the voltametric experiment, HAAH can be viewed either as a TTF derivative with 1,3-dithiole substituents displaying a reversible redox behavior or as dimeric TTP derivative capable of forming the highly reactive HAAH³⁺. Indeed, owing to its hybrid character, HAAH readily yields the stable quasiaromatic radical cation HAAH^{•+} and the dication ⁺HAAH⁺ at relatively low potentials. The formation of the radical trication HAAH³⁺, however, is much less favorable and requires more strenuous conditions.

Conclusion

The oxidation of R-DBTTP (R = H, OCH₃, CF₃) results in the stepwise formation of linearly extended TTF polymers. The polymerization mechanism starts with the formation of the radical cation and proceeds via a fast dimerization reaction to the dicationic protonated TTF derivative. The dimerization rate constants were found to be in the range of $2k_{\text{dim}} = 4 \times 10^6$ to $10^7 \text{ L mol}^{-1} \text{ s}^{-1}$. The dicationic intermediates deprotonate slowly to stable vinylogous TTF derivatives ($k_{\text{H}} = 0.02\text{--}10 \text{ s}^{-1}$). Owing to the presence of two terminal 1,3-dithiole substituents, the dimerization products are capable of forming highly reactive radical trication which can undergo further oligomerization/polymerization steps as discussed above.

References and Notes

- (1) (a) Université Denis Diderot. (b) ESRF. (c) CEA-Grenoble.
- (2) For general reviews, see: (a) Narita, M.; Pittman, C. U. *Synthesis* **1976**, 489. (b) Krief, A. *Tetrahedron* **1986**, *42*, 1209. (c) Schukat, G.; Richter, A. M.; Fanghänel, E. *Sulfur Rep.* **1987**, *7*, 155. (d) Schukat, G.; Fanghänel, E. *Sulfur Rep.* **1993**, *14*, 245. (e) Schukat, G.; Fanghänel, E. *Sulfur Rep.* **1996**, *18*, 1.
- (3) For reviews on the chemistry and physics of TTF based radical salts, see: (a) Ferraro, J. R.; Williams, J. M. *Introduction to Synthetic Organic Conductors*; Academic Press: New York, 1987. (b) Williams, J. M.; Ferraro, J. R.; Thorn, R. J.; Carlson, K. D.; Geiser, U.; Wang, H. H.; Kini, A. M.; Whangbo, M. H. *Organic Superconductors (including Fullerenes)*; Prentice Hall: Englewood Cliffs, NJ, 1992. See also: *J. Mater. Chem.* (Special Issue on Molecular Conductors) **1995**, *5*, 1469–1760.
- (4) (a) Ueno, Y.; Masuyama, Y.; Okawara, M. *Chem. Lett.* **1975**, 603. (b) Pittman, C. U.; Narita, M.; Liang, F. Y. *Macromolecules* **1976**, *9*, 360. (c) Pittman, C. U.; Liang, Y. F.; Ueda, M. *Macromolecules* **1979**, *12*, 541. (d) Kaufman, F. B.; Schroeder, A. H.; Engler, E. M.; Kramer, S. R.; Chambers, J. Q. *J. Am. Chem. Soc.* **1979**, *102*, 483. (e) Kossmehl, G.; Rohde, M. *Macromolecules* **1982**, *9*, 541. (f) Trinh, V. Q.; van Hinh, L.; Schukat, G.; Fanghänel, E. *J. Prakt. Chem.* **1989**, *331*, 826 (g) Frenzel, S.; Arndt, S.; Gregorius, R. M.; Müllen, K. *J. Mater. Chem.* **1995**, *5*, 1529. (h) Yamamoto, T.; Shimizu, T. *J. Mater. Chem.* **1997**, *7*, 1967.
- (5) Müller, H.; Salhi, F.; Divisia-Blohorn, B. *Tetrahedron Lett.* **1997**, *38*, 3215.
- (6) Misaki, Y.; Ohta, T.; Higuchi, N.; Fujiwara, H.; Yamabe, T.; Mori, T.; Mori, H.; Tanaka, S. *J. Mater. Chem.* **1995**, *5*, 1571.
- (7) Adamo, C.; Roger, A.; Scalmani, G.; Müller, H.; Salhi, F.; Barone, V. *J. Phys. Chem. B* **1999**, *103*, 6863.
- (8) (a) Müller, H.; Salhi, F.; Divisia-Blohorn, B.; Genoud, F.; Narayan, T.; Lorenzen, M.; Ferrero, C. *Chem. Comm.* **1999**, 1439. (b) Salhi, F. Ph.D. thesis, Université Joseph Fourier, Grenoble, France, 1999.
- (9) Hapiot, P.; Lorcy, D.; Tallec, A.; Carlier, R.; Robert, A. *J. Phys. Chem.* **1996**, *100*, 14823.
- (10) Garreau, D.; Savéant, J.-M. *J. Electroanal. Chem.* **1972**, *35*, 309.
- (11) (a) Andrieux, C. P.; Garreau, D.; Hapiot, P.; Pinson, J.; Savéant, J.-M. *J. Electroanal. Chem.* **1988**, *321*, 243. (b) Andrieux, C. P.; Hapiot, P.; Savéant, J.-M. *Chem. Rev.* **1990**, *90*, 723.
- (12) By comparison with the peak currents of the reversible wave of the ferrocene/ferricinium couple under the same experimental conditions.
- (13) Since the first wave is irreversible, it is difficult to conclude from this experiment if the second electron transfer is due to a further oxidation of **1** or to the oxidation of electrogenerated intermediates.
- (14) Hansch, C.; Leo, A.; Taft, R. W. *Chem. Rev.* **1991**, *91*, 195.
- (15) Taking the following values for the transfer coefficient $\alpha = 0.5$, for the diffusion coefficient $D = 10^{-5} \text{ cm}^2 \text{ s}^{-1}$. The determined k_s has to be considered as a minimum value because the effects of the residual ohmic drops have not been taken into account.^{11b}
- (16) Kojima, H.; Bard, A. J. *J. Am. Chem. Soc.* **1975**, *97*, 6317.
- (17) A referee suggests based on AM 1 calculations that the dihedral angles for the terminal phenyl substituents of monomer **1** and dimer **4** are approximately 20°, whereas the corresponding value for the internal substituents of **4** amounts to 33°.
- (18) (a) Andrieux, C. P.; Nadjjo, L.; Savéant, J.-M. *J. Electroanal. Chem.* **1973**, *42*, 223. (b) Andrieux, C. P.; Savéant, J.-M.: In *Electrochemical Reactions: Investigation of Rates and Mechanism of Reactions*; Bernasconi, C. F., Ed.; Wiley: New York, 1986; Vol. 6, 4/E, Part. 2, pp 305–390.
- (19) Two protons and two electrons are exchanged when passing from ⁺HAAHHAH⁺ to HAAH²⁺. A detailed discussion regarding the exact nature of the electron transfers involved in the proton abstraction process is beyond the scope of this study.
- (20) In reality, homogeneous electron transfers between the different intermediates could occur and coupling reactions of short-lived radicals such as HAH^{•+} and HAH³⁺ should also take place.
- (21) Genies, E. M.; Bidan, G.; Diaz, A. F. *J. Electroanal. Chem.* **1983**, *149*, 101.
- (22) Bargon, J.; Mohmand, S.; Waltman, R. *IBM J. Res. Dev.* **1983**, *27*, 330. See also: Heinze, J. *Top. Curr. Chem.* **1990**, *152*, 1.